IEEE Access
Multidisciplinary ⋮ Rapid Review ⋮ Open Access Journal

Received 23 December 2022, accepted 13 January 2023, date of publication 23 January 2023, date of current version 26 January 2023.

Digital Object Identifier 10.1109/ACCESS.2023.3238876

RESEARCH ARTICLE

Real-Time Coordinated Control of a Grid-VSC and ESSs in a DC Distribution System for Total Power Loss Reduction Considering Variable Droop Using Voltage Sensitivities

DA-YOUNG SHIN[1], DO-HOON KWON[2], (Member, IEEE), SEUNG-ILL MOON[3], (Senior Member, IEEE), AND YONG-TAE YOON[1], (Member, IEEE)

[1]Department of Electrical and Computer Engineering, Seoul National University, Seoul 08826, South Korea
[2]Department of Electrical and Information Engineering, Seoul National University of Science and Technology, Seoul 01811, South Korea
[3]Institute for Grid Modernization, Korea Institute of Energy Technology (KENTECH), Naju, Jeonnam 58330, South Korea

Corresponding author: Do-Hoon Kwon (dohoonkwon@seoultech.ac.kr)

This work was supported by the Seoul National University of Science and Technology.

ABSTRACT Recent advances in direct current (DC) distribution systems that involve renewable energy sources (RESs) and energy storage systems (ESSs) have shown that DC voltage control improves operational stability. This paper proposes an efficient real-time DC voltage control strategy that reduces total power losses while maintaining the DC voltages within acceptable ranges via coordination of the grid-connected voltage source converter (GVSC) and the ESSs. A new strategy determines whether to invoke cooperative GVSC/ESS control or ESS voltage control alone. The GVSC and ESSs exhibit proportional-integral (PI) and variable droop controllers, respectively. In particular, the variable droop controllers are developed with consideration of the voltage sensitivities. The ESS outputs are then compensated by reference to the droop coefficients and the available ESS output powers. Case studies confirm that our voltage control strategy permits higher minimum DC voltages (and thus smaller total power losses) when consecutive events occur, compared with conventional strategies using PSCAD/EMTDC.

INDEX TERMS DC distribution system, ESS, real-time voltage control, total grid loss, variable droop control, voltage sensitivity, voltage stability.

NOMENCLATURE

A. ACRONYMS

GVSC	Grid connected voltage source converter.
ESS	Energy storage system.
RES	Renewable energy source.
DC	Direct current.
PV	Photovoltaic.
PI	Proportional integral.

B. TOTAL SYSTEM PARAMETERS

V	Index of bus voltage [pu].
P	Indices of the injected real power or ESS power or load power [pu].
L	Index of load.
G	Index of generation (e.g., PV or ESS).
i, j, l	Subscripts for the i-th, j-th or l-th bus.
ESS_j	Subscript for an ESS connected to the j-th bus.
ESS_h	Subscript for the ESS connected h-th bus with the highest voltage sensitivity.
G_{ij}	Sum of DC-line resistances in the intersection set of $\{G_i\}$ and $\{G_j\}$ that is set of line resistances between the i-th or j-th buses and slack bus.
max, min	Superscripts for maximum and minimum of acceptable bus voltage range.
NB, NE	Number of buses and ESSs.

C. GVSC CONTROLLER

up, lo	Superscripts for changing the maximum or minimum of buses to the maximum or minimum of the system.

The associate editor coordinating the review of this manuscript and approving it for publication was Siqi Bu.

D. ESS CONTROLLER

target	Subscript for a target bus (maximum or minimum bus on systems).
sch	Superscript for scheduled.
R	Index of the droop coefficient.
base	Superscript for base droop.
variable	Superscript for variable droop.
*vs, vs**	Superscripts for voltage sensitivity-based droops after and before compensation.
k	Index for voltage sensitivity.
comp	Superscript for compensated output power.

I. INTRODUCTION

Direct current (DC) power sources, such as renewable energy sources (RESs) and energy storage systems (ESSs), have been extensively installed and operated as DC distribution systems [1]; they offer several advantages compared with AC systems, including higher efficiency with fewer power converters, low losses with no skin effects, and high-power quality during blackouts [2]. In DC distribution systems, the DC voltages play an important role in operational stability; neither control synchronization nor reactive power generation is necessary [3]. However, increased numbers of RESs can cause fluctuations in DC voltages that compromise the stabilities of utilities [4], resulting in various problems. For example, an increase in the load current is caused by a decrease in the load voltage, which thus moves away from the optimal point in terms of voltage stability [5]. Furthermore, in the absence of a reserve power margin, large DC voltage fluctuations can reduce the voltage control capacities of photovoltaics or cause disconnection of the wind systems in DC microgrids [6]. Unstable DC voltage fluctuations can cause device malfunctions or other faults in distribution systems [7]. Overall, DC voltage control is important in a DC distribution system that involves RESs. Indeed, there have been several researches on the voltage control strategies in the DC distribution system. For example, the authors of [8] developed an equal loading rate-based control method using a grid-connected voltage source converter (GVSC) to improve voltage control and power sharing within voltage source converter-based DC distribution systems. However,centralized GVSC control was used, rather than distributed control. In [9], an autonomous control strategy using a GVSC, which involved various sources and loads, improved DC voltage stabilities by dividing control into three levels. However, the focus was on the control methods appropriate for different DC voltages, rather than cooperative control. In [10], a cooperative voltage control strategy that involved a distributed generator (DG), a GVSC, and a DG allocation algorithm minimized DG capacity and the operating costs of DC microgrids. In this paper, voltage sensitivity was mainly used to optimize DG allocation in terms of minimizing long-term cost.

Meanwhile, ESSs are important when RESs are integrated with DC distribution systems. ESSs manage the voltage sags that can be attributed to the inevitable energy supply volatilities of RESs or instantaneous faults [11]. Thus, ESSs enhance the voltage stabilities of RES-containing DC distribution systems. Many operators use ESS utilities to control DC voltages autonomously using ESS powers/energies when the voltage fluctuates [9]. Therefore, many researchers have studied DC voltage control of DC distribution systems with ESSs. Genetic algorithm-based ESS scheduling has been used to control voltage considering RES fluctuations in DC distribution systems [12]. However, that work focused on ESS scheduling without real-time voltage control. Several papers have been proposed on explored real-time voltage control in DC distribution systems [13], [14]. In [13], an autonomous ESS PI controller (a combination of double closed-loop and current-sharing controllers) reduced DC voltage fluctuations in islanded DC microgrids with PVs and ESSs. In [14], two adaptive droop controllers for ESSs maintained DC voltages and eliminated current-sharing errors in DC microgrids. However, these studies did not focus on cooperative control by a GVSC and ESSs. A few studies used such coordinated control to maintain DC voltages [15], [16]. For example, in [15], a multi-agent control strategy (using a GVSC and ESSs) improved voltage stability by allocating optimal active powers to the ESSs of DC microgrids. In [16], an autonomous droop controller for a GVSC and the ESSs regulated the DC voltages of DC microgrids. In this paper, the droop coefficients applied to the GVSC and ESSs differed when operation was normal or islanded. However, the available ESS output powers and the voltage sensitivities needed to reduce the total power loss were not considered.

This paper proposes a new real-time coordinated control strategy for a GVSC and ESSs in a DC distributed system to reduce total power loss and to improve voltage stability by operating within the acceptable voltage range. The new strategy changes reference signals of ESS and GVSC instantaneously, not predetermined scheduling signals, based on DC system conditions. Specifically, voltage sensitivities are utilized for voltage controllers in the GVSC and ESSs. PI and variable droop controllers are included in the GVSC and ESSs, respectively. The voltage sensitivities are used to calculate appropriate droop coefficients. The compensated ESS output reference values for real-time voltage control are obtained based on the droop coefficients and the available ESS output powers. Compared with conventional voltage strategies, our voltage control strategy enables greater increases in the DC voltages associated with lower total power loss when consecutive events occur (e.g., PV faults and load increases). Furthermore, a new operating strategy determines whether to invoke cooperative GVSC/ESS voltage control or ESS voltage control alone. The method is applied to the modified IEEE-13-bus system; effectiveness is verified using PSCAD/EMTDC which utilized to simulate various real-time control methods [17], [18], [19], [20].

The main contributions of this paper are summarized below:

•This paper proposes a new real-time voltage control system that reduces total power loss via coordination of the GVSC and ESSs, with consideration of the voltage sensitivities of a DC distributed system.

•Variable droop coefficients for the ESSs based on the voltage sensitivities and compensated ESS powers considering ESS capacities are also developed. These arrangements enable the maintenance of higher DC voltages and lower total power loss when consecutive events occur.

•A new operating strategy chooses between coordinated control by the GVSC and ESSs or ESS control alone.

The rest of the paper is organized as follows. Section II describes our voltage control strategy. Section III presents the three required modules. Section IV contains the simulations, and Section V presents the conclusion.

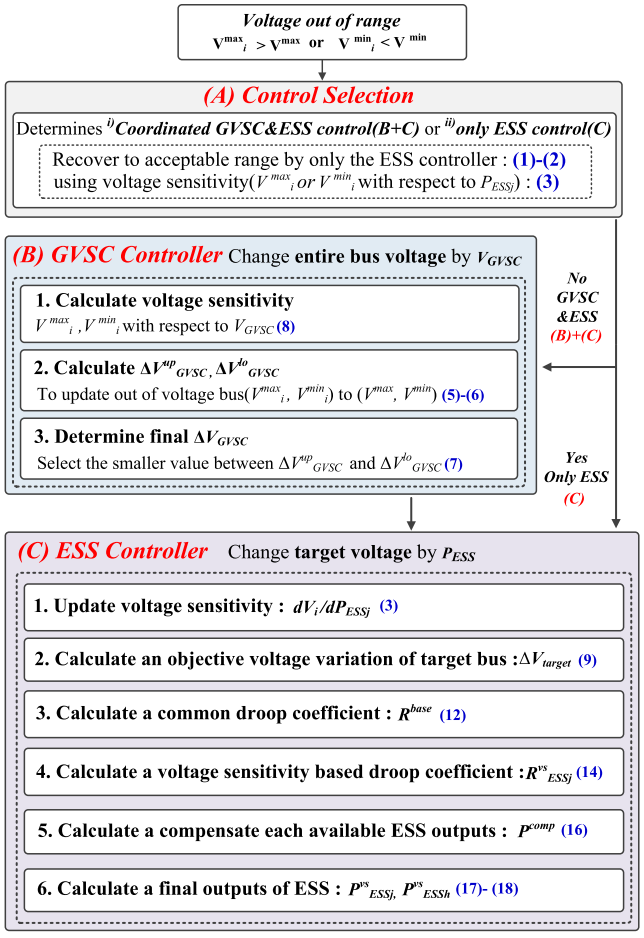

FIGURE 1. Schematic diagram of the proposed real-time coordinated control strategy for a GVSC and ESSs.

II. A NEW VOLTAGE CONTROL STRATEGY USING THE GVSC AND ESSs OF A DC DISTRIBUTION SYSTEM

Fig. 1 shows a schematic diagram of our strategy. The three modules are (a) a control-selection, (b) a GVSC controller, and (c) an ESS controller. When the i-th bus voltage (V_i) of the DC distribution system is out of the acceptable range, the control-selection module determines whether the GVSC/ESS or the ESS should be used to restore V_i to an acceptable range by considering the voltage sensitivities of the i-th bus to the output powers of the ESSs. If the module calculates that V_i cannot recover using only ESS control, the strategy regulates all bus voltages using the GVSC controller; this adjusts the GVSC voltage (V_{GVSC}) until the maximum bus voltage (V_i^{max}) or minimum bus voltage (V_i^{min}) is the maximum acceptable voltage (V^{max}) or minimum acceptable voltage (V^{min}), respectively, based on the voltage sensitivity of V_i^{max} or V_i^{min} to V_{GVSC} (see Section III-B).

The ESS controller adjusts the ESS output powers either after the GVSC controller completes regulation of V_{GVSC}, or when V_i^{max} or V_i^{min} recovers to within an acceptable range through use of the ESS controller alone. Specifically, the ESS controller calculates a common V-P droop coefficient (R^{base}) for each ESS in the DC distribution system by reference to either V_i^{max} or V_i^{min}. The voltage sensitivities of all ESSs to all bus voltages are obtained using the scheduled and measured bus voltages, the output powers of the ESSs, and the resistances of the DC-lines in the DC distribution system. Subsequently, each ESS is assigned a modified droop coefficient (R^{vs}) (from the R^{base}) that reflects the voltage sensitivities of that ESS to V_i^{max} or V_i^{min}. Thus, in each ESS, the R^{vs} considers the unique voltage sensitivities of that ESS. The ESS controller calculates the R^{vs} of each ESS at each simulation time-step, allowing the ESSs to control the system voltage in real-time. Finally, each ESS regulates the output power via R^{vs}.

III. THE THREE MODULES FOR THE PROPOSED VOLTAGE CONTROL STRATEGY

A. CONTROL SELECTION

The control selection module determines whether coordinated GVSC and ESS control or ESS control alone is used to restore V_i^{max} or V_i^{min} to within the acceptable range. To ensure accurate operation, it is assumed that the system operator continuously measures all bus voltages and that DC system data (e.g., the resistances of DC-lines) are available [21]. When V_i^{max} or V_i^{min} becomes larger or smaller than V^{max} or V^{min}, respectively, and does not recover to within the acceptable range using the ESS controller alone, coordinated GVSC and ESS control is selected as follows:

$$V^{min} - V_i^{min} < \sum_{j=1}^{NE} \frac{dV_i^{min}}{dP_{ESS_j}} \Delta P_{ESS_j} \tag{1}$$

$$\sum_{j=1}^{NE} \frac{dV_i^{max}}{dP_{ESS_j}} \Delta P_{ESS_j} < V^{max} - V_i^{max} \tag{2}$$

In (1) and (2), the bus voltage sensitivities according to the ESS output powers are calculated using the G matrices of the simulation time-steps [5]:

$$\frac{dV_i}{dP_{ESS_j}} \cong \frac{V_i^2}{(V_i^2 + G_{ii}P_i)V_j}\left(G_{ij} - \sum_{l=1, l\neq i}^{NB} \frac{G_{il}G_{lj}P_l}{V_l^2 + G_{ll}P_l}\right) \tag{3}$$

$$P_i = P_{G_i} - P_{L_i} \tag{4}$$

where G_{ij} is the sum of DC-line resistances in the intersection set of $\{G_i\}$ and $\{G_j\}$ that is set of line resistances between the i-th or j-th buses and slack bus.

B. GVSC CONTROLLER

If the control selection module chooses coordinated GVSC and ESS control, the GVSC controller operates first to change all bus voltages to within acceptable ranges and reduces the total power loss by regulating V_{GVSC}. Specifically, the GVSC controller calculates ΔV^{up}_{GVSC} and ΔV^{lo}_{GVSC}, such that V_i^{max} and V_i^{min} in the distribution system become V^{max} and V^{min}, respectively, using the voltage sensitivities of V_i^{max} and V_i^{min} to V_{GVSC}:

$$\Delta V^{up}_{GVSC} = \min(\left|V^{max} - V_i^{max}\right| / \frac{dV_i^{max}}{dV_{GVSC}}, \left|V^{max} - V_{GVSC}\right|) \tag{5}$$

$$\Delta V^{lo}_{GVSC} = \min(\left|V^{min} - V_i^{min}\right| / \frac{dV_i^{min}}{dV_{GVSC}}, \left|V^{min} - V_{GVSC}\right|) \tag{6}$$

The GVSC controller then selects the smaller of ΔV^{up}_{GVSC} and ΔV^{lo}_{GVSC} to be ΔV_{GVSC}, while regulating V_{GVSC} up to ΔV_{GVSC}:

$$\Delta V_{GVSC} = \min(\Delta V^{up}_{GVSC}, \Delta V^{lo}_{GVSC}) \tag{7}$$

The ESSs contribute as much power as possible to minimize total power loss below the acceptable voltage range during coordinated control of the GVSC and ESSs. According to (5) and (6), the voltage sensitivities of V_i^{max} and V_i^{min} to V_{GVSC} are expressed in (8) [5]:

$$\frac{dV_i}{dV_{GVSC}} \cong \frac{V_i^2}{V_i^2 + G_{ii}P_i}(1 - \sum_{l=1,l\neq i}^{NB} \frac{G_{il}P_l}{V_l^2 + G_{ll}P_l}) \tag{8}$$

We focus on reduction of the total power loss; we do not consider restoration of excessive voltage to within the acceptable range using the GVSC controller alone [22].

C. ESS CONTROLLER

The ESS controller regulates the voltages of a target bus (V_{target}) and nearby buses. The target bus can be the maximum- or minimum-voltage bus in the system. When the control-selection module invokes the ESS controller either directly or after the GVSC controller has operated, the ESS controller calculates the objective voltage variation of the target bus that can be regulated by the ESS outputs. The objective voltage variation is the difference between the scheduled and measured voltages of the target bus:

$$\Delta V_{target} = V^{sch}_{target} - V_{target} \tag{9}$$

In the conventional strategy, each ESS in the DC system regulates its own output power by reference to an individual droop coefficient derived using the V^{min} (or V^{max}), the scheduled voltage of the target bus (V^{sch}_{target}), and its available output power (10) [23]. Note that the available power of each ESS differs in terms of the maximum (or minimum) and the scheduled output power (i.e., $P_{ESS}^{max(min)} - P_{ESS}^{sch}$); this ensures scheduled operation of all ESSs after an abnormal condition is cleared.

$$\frac{1}{R^{variable}_{ESS_j}} = \frac{1}{\left|\frac{V^{min(max)} - V^{sch}_{target}}{P^{max(min)}_{ESS_j} - P^{sch}_{ESS_j}}\right|} \tag{10}$$

Each ESS output power is thus calculated as in (11) and is usually updated at each scheduling time-step which are several minutes [23], [24].

$$P^{variable}_{ESS_j} = P^{sch}_{ESS_j} - \Delta V_{target} \times \frac{1}{R^{varialbe}_{ESS_j}} \tag{11}$$

In proposed strategy, all ESSs adjust their output powers based on their voltage sensitivities to achieve objective voltage variation. To determine the output power variations of all ESSs (ΔP_{ESSj}), a common droop coefficient (R_{base}) is first created using V^{max} or V^{min}, V^{sch}_{target}, and the summed available output powers of the ESSs (12):

$$\frac{1}{R^{base}} = \frac{1}{\left|\frac{V^{min(max)} - V^{sch}_{t\,\mathrm{arg}\,et}}{(P^{max(min)}_{ESS_1} + \cdots + P^{max(min)}_{ESS_N}) - (P^{sch}_{ESS_1} + \cdots + P^{sch}_{ESS_N})}\right|} \tag{12}$$

Each ESS droop coefficient (R^{VS}_j) is then modified using the common droop coefficient by reference to the proportion of voltage sensitivity imposed by the target bus voltage, as expressed in (13) and (14). Each ESS output power can be calculated as in (15). Note that this process is repeated at each time-step which are several seconds, which is sufficiently close to control voltages in real-time [25].

$$\frac{dV_{target}}{dP_{ESS_1}} : \cdots : \frac{dV_{target}}{dP_{ESS_{NE}}} = \Delta P_{ESS_1} : \cdots : \Delta P_{ESS_{NE}} = k_1 : \cdots : k_{ESS_{NE}} \tag{13}$$

$$\frac{1}{R^{vs}_{ESS_j}} = \frac{k_{ESS_j}}{k_1 + \cdots + k_{ESS_{NE}}} \frac{1}{R^{base}} \tag{14}$$

$$P^{vs*}_{ESS_j} = P^{sch}_{ESS_j} - \Delta V_{target} \times \frac{1}{R^{vs}_{ESS_j}} \tag{15}$$

The ESS output power (15) means that an ESS that is more sensitive to the voltage of the target bus can more efficiently regulate the power output needed to restore the target bus voltage to within the acceptable range. Thus, the summed ESS output variation is lower than the variation of the summed possible ESS power output. However, the total power loss when ESS output is regulated by Eq. (15) may be larger than the total power loss of the conventional strategy (11).

To reduce the total power loss over the acceptable voltage range, our strategy compensates for the output powers of ESSs for which the target bus voltage sensitivities are maximal (i.e., for the ESS_h values that consider the maximal ESS

power outputs). The compensated output power of an ESS_h is the difference between the maximum and calculated output powers. We set the compensated ESS_h output power to 10% of the available output power for the next scheduled operation, as follows:

$$P^{comp} = \sum_{l=1}^{NE} \left(P^{max}_{ESS_l} - P^{vs*}_{ESS_l}\right) \times 10\% \tag{16}$$

The final output powers of all ESSs are the summed powers of (15) with the modified compensated powers of (16) that consider the effects of the powers on the sensitivity of the target bus voltage, as expressed in (17) and (18):

$$P^{vs}_{ESS_j} = P^{sch}_{ESS_j} - \Delta V_{target} \times \frac{1}{R^{vs}_{ESS_j}} \tag{17}$$

$$P^{vs}_{ESS_h} = P^{sch}_{ESS_h} - \Delta V_{target} \times \frac{1}{R^{vs}_{ESS_h}} + P^{comp} \times \frac{k_{ESS_h}}{k_1 + \cdots + k_{ESS_{NE}}} \tag{18}$$

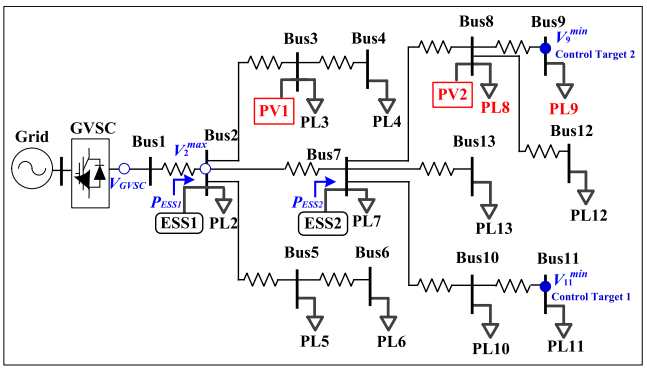

FIGURE 2. Test distributed DC system: IEEE 13 bus modified.

TABLE 1. Parameters for the test system.

Devices	Parameters	Values	Descriptions
DC distribution system	V_{rated} [V]	400	Nominal DC voltages
	V^{max}, V^{min} [pu]	1.05, 0.95	Maximum and minimum voltage
	P_{rated} [MW]	1	Nominal system power
ESS	$P^{max}{}_{ESS1}$, $P^{max}{}_{ESS2}$ [kW]	250, 180	Maximum output of ESSs
	$P^{min}{}_{ESS1}$, $P^{min}{}_{ESS2}$ [kW]	-250, -180	Minimum output of ESSs
PV	P_{PV1}, P_{PV2} [MW]	0.6, 1.2	Capacity of PV

IV. CASE STUDIES AND RESULTS

A. TEST SYSTEM AND SIMULATION CONDITIONS

This paper implemented new control strategy using PSCAD/EMTDC which utilized to verify various real-time control methods. Fig. 2 shows the test distributed DC system, which was modified by including aspects of the IEEE 13-bus system [26]. The GVSC works at Bus 1; two ESSs are connected to Buses 2 and 7. The ESS powers are 250 and 180 kW [27], [28]. There are also 0.6 MW- and 1.2 MW-rated PVs in the test system connected to Buses 3 and 8, respectively [29]. The DC power and voltage are 1 MW and 400 V, respectively [30]. The test system operates with constant scheduled and time-varying reference values of V_{GVSC} and P_{ESS} under abnormal conditions (i.e., real-time control situation). Prior to real-time voltage control, all loads and PVs were forecasted at 15-min intervals. The GVSC voltage and ESS output powers (V^{sch}_{GVSC} and P^{sch}_{ESS}) were scheduled based on these values [31]. At 2-s intervals [32], [33], [34], [35], all loads and PVs were measured; the GVSC and ESS reference values were updated accordingly (i.e., real-time voltage control). We extracted the load profiles during such control from the overall 2021 Korean load profile [36]. Table 1 lists the ESSs, PVs, and test system parameters.

Table 2 lists the principal aspects of the new (Case 1) and conventional (Cases 2 and 3) strategies used for real-time voltage control of DC distribution systems. Both consider the available ESS output powers ((11) and (15), respectively); Case 2 controls DC voltages using variable droops alone, whereas voltage sensitivities, such as the sensitivities in (13), are not involved. We compared Cases 1 and 2 to determine the effects of sensitivity-based voltage control on real-time voltage control (Sections III-B and C). Case 3 involves the commonly used coordinated GVSC and ESS control (i.e., a constant droop voltage controller) [3]. Fig. 3 shows the variations of the total loads in the DC distribution system. All loads increase dramatically at $t = 2$ s, but only the loads of buses 8 and 9 rapidly increase at $t = 10$ s. In terms of real-time voltage control, both PVs were assumed to be disconnected at $t = 2$ s.

TABLE 2. Aspects of the New and conventional control strategies.

Strategies		Model	Voltage sensitivity	Power range
Pro.	Case 1	Voltage sensitivity-based droop	O	O
Conv.	Case 2	Variable droop	X	O
	Case 3	Constant droop	X	X

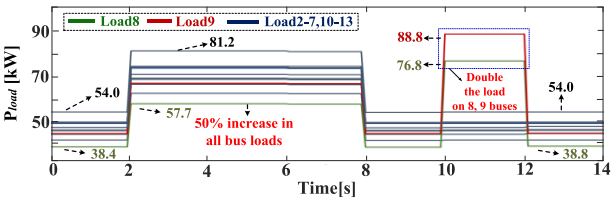

FIGURE 3. Real time total load profile of the test system.

B. SIMULATION RESULTS

Fig. 4 and Table 3 compares the maximum and minimum DC voltages of the test system using the new (Case 1) and conventional strategies (Cases 2 and 3). Note that the 2-Bus

voltage V_2^{max} was the maximum, whereas the 11-Bus voltage V_{11}^{min} was the minimum, until $t = 10$ s in all case studies. Before $t = 2$ s, both voltages were maintained at the initial voltages. They decreased after $t = 2$ s because all PVs were disconnected and all loads began to increase at $t = 2$ s, as shown in Fig. 3. In particular, the minimum DC voltage decreased below the acceptable range (i.e., V^{min}) immediately after $t = 2$ s, as shown in Fig. 4(b); this activated real-time voltage control.

The control-selection module selected coordinated control by the GVSC and ESSs because the minimum voltage could not be restored to within the acceptable range using the ESS controller alone; (1) was not satisfied. The GVSC controller increased V_{GVSC} from 1.03 pu to 1.05 pu at $t = 3$ s, as shown in Fig. 5; this change increased all DC voltages, including the maximum and minimum voltages. Note that V_{GVSC} values for Cases 1–3 were identical to V^{max} values because V_{GVSC} was limited to V^{max} for all cases, although the GVSC controller of Case 1 calculated ΔV_{GVSC} as 0.065 pu using (5)–(8).

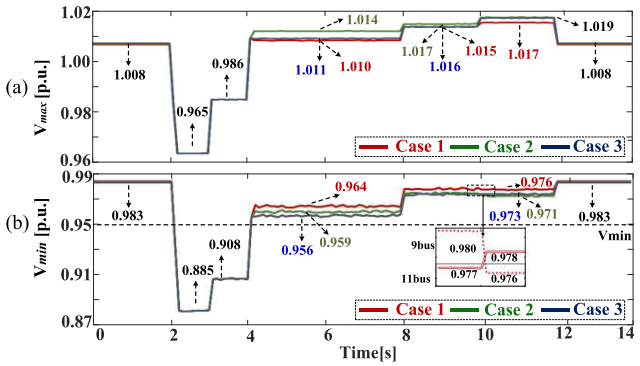

FIGURE 4. Maximum and minimum voltage: (a) V_{max}, (b) V_{min}.

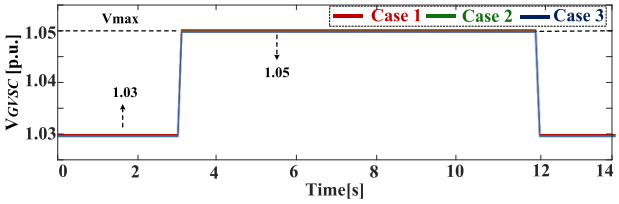

FIGURE 5. Voltage of GVSC.

TABLE 3. Maximum and minimum DC voltage during 4s - 12s.

		V^{max}			V^{min}		
		4s–8s	8s–10s	10s–12s	4s–8s	8s–10s	10s–12s
Pro.	Case 1	1.010	1.015	1.017	0.964	0.977	0.976
Conv.	Case 2	1.014	1.017	1.019	0.959	0.974	0.971
	Case 3	1.011	1.016	1.019	0.956	0.972	0.973

After operation of the GVSC controller, the ESS controller restored the minimum voltage to within the acceptable range at $t = 4$ s. Fig. 6 compares the total ESS output powers of Cases 1–3. In Case 1, the total ESS output increased to 200.2 kW, whereas it attained 265.3 and 218.8 kW in Cases 2 and 3, respectively; the new strategy regulates the ESS output powers more efficiently, compared with conventional strategies that use droop coefficients based on the voltage sensitivities (i.e., (12)–(15)). Fig. 7 shows the ESS droop coefficients for Cases 1–3. For Case 1, the droop coefficients of ESS1 and ESS2 were higher and lower than the droop coefficients of Cases 2 and 3, respectively. This effectively allocated the ESS output powers; total power use was reduced. Although the total ESS output power of Case 1 was less than the total ESS output powers of the other Cases, the minimum voltage of Case 1 increased to 0.964 pu; this was higher than the minimum voltages of cases 2 and 3 (0.959 pu and 0.956 pu, respectively). However, the maximum voltage of Case 1 (1.010 pu) was smaller than the maximum voltages of Cases 2 and 3 (1.104 pu and 1.011 pu, respectively), as shown in Fig. 4 and Table 3. Thus, the power loss of Case 1 was 42.0 kW from $t = 4$ s to $t = 8$ s, as shown in Fig. 8. In contrast, for Cases 2 and 3, the power losses during the same period were 42.9 and 46.5 kW, respectively.

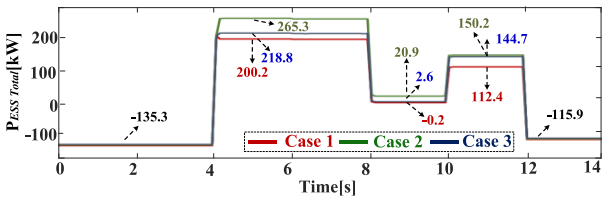

FIGURE 6. Total outputs of ESS.

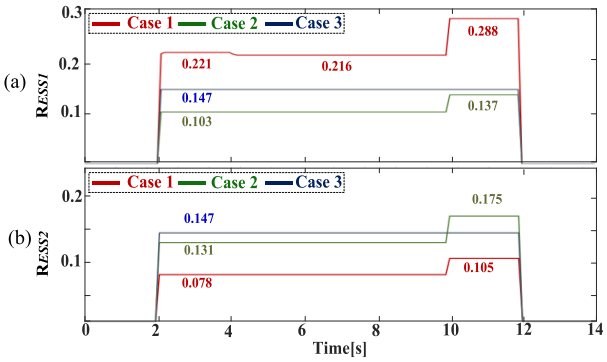

FIGURE 7. Droop coefficient: (a) R_{ESS1}, (b) R_{ESS2}.

Subsequently, all loads decreased by 50% at $t = 8$ s, which caused the maximum and minimum voltages to increase. Although these voltages remained within the acceptable ranges, the GVSC and ESS controllers continued to operate to reduce the total power loss. In particular, the total ESS output power decreased to –0.2 kW in Case 1, but the powers were 20.9 and 2.6 kW for Cases 2 and 3, respectively; the output powers of ESS1 and ESS2 in Case 1 were –40.2 kW and 40.0 kW, respectively, using the droop coefficients based

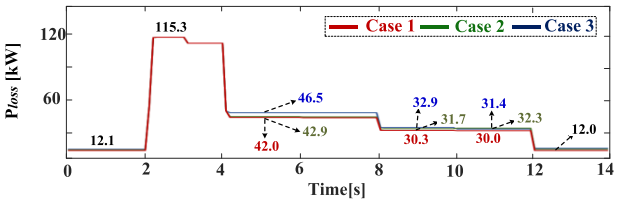

FIGURE 8. Total power losses.

on the voltage sensitivities. However, the minimum voltage of Case 1 (0.977 pu) was higher than the minimum voltages of Cases 2 and 3 (0.974 pu and 0.972 pu, respectively), as shown in Fig. 4(b) and Table 3. This resulted in a smaller total power loss for Case 1 (30.3 kW) than for Cases 2 and 3 (31.7 and 32.9 kW, respectively), as shown in Fig. 8. Note that V_{GVSC} was maintained at 1.05 pu in all cases; this was the V^{max} limit.

The minimum voltage changed from the 11-Bus voltage to the 9-Bus voltage after $t = 10$ s (i.e., V_9^{min}); the ESS droop coefficients of Cases 1 and 2 also varied, as shown in Fig. 7, because only the 8- and 9-Bus loads increased (to 76.8 and 88.8 kW, respectively) at $t = 10$ s. Because the ESS droop coefficients consider the voltage sensitivities, the maximum and minimum voltages of Case 1 were lower and higher, respectively, than the maximum and minimum voltages of Cases 2 and 3, as indicated in Table 3. However, the total ESS power of Case 1 remained smaller than the total ESS powers of Cases 2 and 3, as shown in Fig. 6. As indicated in Table 4, Case 1 reduced the total ESS output power over 4–12s by 36.5 % and 13.9 % (compared with the total ESS output powers of Cases 2 and 3, respectively) and the summed total power loss over this time by 3.7% and 8.9% using real-time voltage control. Compared with conventional strategies, the new strategy reduces the total power loss by using less ESS energy through the application of real-time voltage control.

TABLE 4. Total ESS outputs and system losses.

P_{ESS}, P_{loss} over 4s-12s [kW]	Total outputs of ESS				Total power loss	
	(1) P_{ESS1}	(2) P_{ESS2}	(1)+(2)	((b)-(a))/(a) or ((c)-(a))/(a)	(3) P_{loss} [kW]	((b)-(a))/(a) or ((c)-(a))/(a)
Case 1(a)	-11.7	1026.0	1014.3	-	291.5	-
Case 2(b)	845.7	538.5	1384.2	36.5%	302.3	3.7%
Case 3(c)	582.7	572.1	1154.9	13.9%	317.4	8.9%

V. CONCLUSION

This paper proposed an efficient real-time DC voltage control strategy for DC distribution systems that reduces the total power loss while maintaining the DC voltages within acceptable ranges through coordination between the GVSC and ESSs. PI and variable droop controllers were integrated into the GVSC and ESSs, respectively. Appropriate droop coefficients were calculated with consideration of the voltage sensitivities. Compensated ESS output reference values for real-time voltage control were obtained using these droop coefficients and the available ESS output powers. This process allowed the ESSs to restore DC voltages to within acceptable ranges using less ESS power than the conventional strategies, leading to improvement of voltage stability and smaller total power losses when consecutive events occurred. Additionally, this paper proposes an operating strategy that determines whether to activate cooperative GVSC and ESS voltage control or ESS control alone. Simulations performed using PSCAD/EMTDC showed that, compared with conventional control, our strategy reduced the total ESS output powers by 13.9–36.5% and the total power losses by 3.7–8.9% when real-time voltage control was invoked. This confirmed that the proposed strategy can reduce the total power loss effectively utilizing less ESS energy during the real-time voltage control. Future work will focus on online verification of the proposed strategy.

REFERENCES

[1] J. J. Justo, F. Mwasilu, J. Lee, and J.-W. Jung, "AC-microgrids versus DC-microgrids with distributed energy resources: A review," *Renew. Sustain. Energy Rev.*, vol. 24, pp. 387–405, Aug. 2013.
[2] D. Kumar, F. Zare, and A. Ghosh, "DC microgrid technology: System architectures, AC grid interfaces, grounding schemes, power quality, communication networks, applications, and standardizations aspects," *IEEE Access*, vol. 5, pp. 12230–12256, 2017.
[3] Y. Li, L. He, F. Liu, C. Li, Y. Cao, and M. Shahidehpour, "Flexible voltage control strategy considering distributed energy storages for DC distribution network," *IEEE Trans. Smart Grid*, vol. 10, no. 1, pp. 163–172, Jan. 2019.
[4] K. R. Bharath, C. Harsha, and P. Kanakasabapathy, "Control of bidirectional DC-DC converter in renewable based DC microgrid with improved voltage stability," *Int. J. Renew. Energy Res.*, vol. 8, no. 2, pp. 871–877, 2018.
[5] H.-Y. Jeong, J.-C. Choi, D.-J. Won, S.-J. Ahn, and S.-I. Moon, "Formulation and analysis of an approximate expression for voltage sensitivity in radial DC distribution systems," *Energies*, vol. 8, no. 9, pp. 9296–9319, Aug. 2015.
[6] F. S. Al-Ismail, "DC microgrid planning, operation, and control: A comprehensive review," *IEEE Access*, vol. 9, pp. 36154–36172, 2021.
[7] G. S. Rawat and S. Suhag, "Survey on DC microgrid architecture, power quality issues and control strategies," in *Proc. 2nd Int. Conf. Inventive Syst. Control (ICISC)*, Jan. 2018, pp. 500–505.
[8] Y. Wang, J. He, Y. Zhao, G. Liu, J. Sun, H. Li, and C. Wang, "Equal loading rate based master–slave voltage control for VSC based DC distribution systems," *IEEE Trans. Power Del.*, vol. 35, no. 5, pp. 2252–2259, Oct. 2020.
[9] D. Chen, L. Xu, and L. Yao, "DC voltage variation based autonomous control of DC microgrids," *IEEE Trans. Power Del.*, vol. 28, no. 2, pp. 637–648, Apr. 2013.
[10] J.-C. Choi, H.-Y. Jeong, J.-Y. Choi, D.-J. Won, S.-J. Ahn, and S.-I. Moon, "Voltage control scheme with distributed generation and grid connected converter in a DC microgrid," *Energies*, vol. 7, no. 10, pp. 6477–6491, Oct. 2014.
[11] C. Zhang, P. Li, and Y. Guo, "Bidirectional DC/DC and SOC drooping control for DC microgrid application," *Electronics*, vol. 9, no. 2, p. 225, Jan. 2020.
[12] B. Ko, N. Utomo, G. Jang, J. Kim, and J. Cho, "Optimal scheduling for the complementary energy storage system operation based on smart metering data in the DC distribution system," *Energies*, vol. 6, no. 12, pp. 6569–6585, Dec. 2013.
[13] Q. Yang, L. Jiang, H. Zhao, and H. Zeng, "Autonomous voltage regulation and current sharing in islanded multi-inverter DC microgrid," *IEEE Trans. Smart Grid*, vol. 9, no. 6, pp. 6429–6437, Nov. 2018.
[14] M. Mokhtar, M. I. Marei, and A. A. El-Sattar, "An adaptive droop control scheme for DC microgrids integrating sliding mode voltage and current controlled boost converters," *IEEE Trans. Smart Grid*, vol. 10, no. 2, pp. 1685–1693, Mar. 2019.

[15] T. Morstyn, B. Hredzak, and V. G. Agelidis, "Cooperative multi-agent control of heterogeneous storage devices distributed in a DC microgrid," *IEEE Trans. Power Syst.*, vol. 31, no. 4, pp. 2974–2986, Jul. 2016.
[16] D. Chen and L. Xu, "Autonomous DC voltage control of a DC microgrid with multiple slack terminals," *IEEE Trans. Power Syst.*, vol. 27, no. 4, pp. 1897–1905, Nov. 2012.
[17] X. Feng, K. L. Butler-Purry, and T. Zourntos, "Multi-agent system-based real-time load management for all-electric ship power systems in DC zone level," *IEEE Trans. Power Syst.*, vol. 27, no. 4, pp. 1719–1728, Nov. 2012.
[18] T. Liu, W. Pan, R. Quan, and M. Liu, "A variable droop frequency control strategy for wind farms that considers optimal rotor kinetic energy," *IEEE Access*, vol. 7, pp. 68636–68645, 2019.
[19] Q. Zhou, Z. Tian, M. Shahidehpour, X. Liu, A. Alabdulwahab, and A. Abusorrah, "Optimal consensus-based distributed control strategy for coordinated operation of networked microgrids," *IEEE Trans. Power Syst.*, vol. 35, no. 3, pp. 2452–2462, May 2020.
[20] S. F. Zarei, H. Mokhtari, M. A. Ghasemi, and F. Blaabjerg, "Reinforcing fault ride through capability of grid forming voltage source converters using an enhanced voltage control scheme," *IEEE Trans. Power Del.*, vol. 34, no. 5, pp. 1827–1842, Oct. 2019.
[21] C. N. Papadimitriou, E. I. Zountouridou, and N. D. Hatziargyriou, "Review of hierarchical control in DC microgrids," *Electr. Power Syst. Res.*, vol. 122, pp. 159–167, May 2015.
[22] B. Liu, F. Zhuo, Y. Zhu, and H. Yi, "System operation and energy management of a renewable energy-based DC micro-grid for high penetration depth application," *IEEE Trans. Smart Grid*, vol. 6, no. 3, pp. 1147–1155, May 2015.
[23] C. Wang, J. Meng, Y. Wang, and H. Wang, "Adaptive virtual inertia control for DC microgrid with variable droop coefficient," in *Proc. 20th Int. Conf. Electr. Mach. Syst. (ICEMS)*, Aug. 2017, pp. 1–5.
[24] Y. Liu, S. Xie, H. Liang, and H. Cui, "Coordinated control strategy of multi-terminal VSC-HVDC system considering frequency stability and power sharing," *IET Gener., Transmiss. Distrib.*, vol. 13, no. 22, pp. 5188–5196, Oct. 2019.
[25] J. Meng, Y. Wang, C. Wang, and H. Wang, "Design and implementation of hardware-in-the-loop simulation system for testing control and operation of DC microgrid with multiple distributed generation units," *IET Gener. Transmiss. Distrib.*, vol. 11, no. 12, pp. 3065–3072, Aug. 2017.
[26] W. H. Kersting, "Radial distribution test feeders," *IEEE Trans. Power Syst.*, vol. 6, no. 3, pp. 975–985, Aug. 1991.
[27] J. Liu, T. Jin, L. Liu, Y. Chen, and K. Yuan, "Multi-objective optimization of a hybrid ESS based on optimal energy management strategy for LHDs," *Sustainability*, vol. 9, no. 10, p. 1874, Oct. 2017.
[28] L. de Oliveira-Assis, P. García-Trivino, E. P. P. Soares-Ramos, R. Sarrias-Mena, C. A. García-Vázquez, C. E. Ugalde-Loo, and L. M. Fernández-Ramírez, "Optimal energy management system using biogeography based optimization for grid-connected MVDC microgrid with photovoltaic, hydrogen system, electric vehicles and Z-source converters," *Energy Convers. Manag.*, vol. 248, pp. 1–14, Nov. 2021.
[29] A. Maknouninejad, Z. Qu, F. L. Lewis, and A. Davoudi, "Optimal, nonlinear, and distributed designs of droop controls for DC microgrids," *IEEE Trans. Smart Grid*, vol. 5, no. 5, pp. 2508–2516, Sep. 2014.
[30] B. Wang, M. Sechilariu, and F. Locment, "Intelligent DC microgrid with smart grid communications: Control strategy consideration and design," *IEEE Trans. Smart Grid*, vol. 3, no. 4, pp. 2148–2156, Dec. 2012.
[31] S. S. Reddy, P. R. Bijwe, and A. R. Abhyankar, "Real-time economic dispatch considering renewable power generation variability and uncertainty over scheduling period," *IEEE Syst. J.*, vol. 9, no. 4, pp. 1440–1451, Dec. 2015.
[32] J.-K. Kim, S. Lee, J.-S. Kim, and H. Choi, "The need for modeling the impact of behind-the-meter generation trip on primary frequency response through operational experiences in Korea power system," *IEEE Trans. Power Syst.*, vol. 37, no. 2, pp. 1661–1664, Mar. 2022.
[33] S. Nowak, N. Tehrani, M. S. Metcalfe, W. Eberle, and L. Wang, "Cloud-based DERMS test platform using real-time power system simulation," in *Proc. IEEE Power Energy Soc. Gen. Meeting (PESGM)*, Aug. 2018, pp. 1–5.
[34] S. Xia, S. Bu, X. Luo, K. W. Chan, and X. Lu, "An autonomous real-time charging strategy for plug-in electric vehicles to regulate frequency of distribution system with fluctuating wind generation," *IEEE Trans. Sustain. Energy*, vol. 9, no. 2, pp. 511–524, Apr. 2018.
[35] W. Wei, N. Li, J. Wang, and S. Mei, "Estimating the probability of infeasible real-time dispatch without exact distributions of stochastic wind generations," *IEEE Trans. Power Syst.*, vol. 31, no. 6, pp. 5022–5032, Nov. 2016.
[36] *Electric Power Statistics Information System*. [Online]. Available: https://epsis.kpx.or.kr/epsisnew/selectEkgeEpsMepRealChart.do?menuId=030300

DA-YOUNG SHIN received the B.S. and M.S. degrees in electrical engineering from Seoul National University, in 2011 and 2013, respectively, where she is currently pursuing the Ph.D. degree in electrical and computer engineering. She is currently working as a Senior Researcher with the Korea Institute of Energy Technology Evaluation and Planning. Her research interests include the dc distribution systems, power system economics, and smart grid.

DO-HOON KWON (Member, IEEE) received the B.S., M.S., and Ph.D. degrees in electrical engineering from Seoul National University, Seoul, South Korea, in 2010, 2012, and 2018, respectively. From 2018 to 2021, he worked as a Senior Researcher with the Korea Electrotechnology Research Institute (KERI). He is currently working as an Assistant Professor with the Department of Electrical and Information Engineering, Seoul National University of Science and Technology. His research interests include HVdc systems, renewable energy integration in power systems, and smart power networks. He was selected as a recipient of the Best Reviewer Award for the IEEE TRANSACTIONS ON SMART GRID, in 2017.

SEUNG-ILL MOON (Senior Member, IEEE) received the B.S. degree in electrical engineering from Seoul National University, Seoul, South Korea, in 1985, and the M.S. and Ph.D. degrees in electrical engineering from The Ohio State University, Columbus, OH, USA, in 1989 and 1993, respectively. He is currently a Professor with the Korea Institute of Energy Technology (KENTECH). His research interests include power system operations, power quality, HVdc systems, renewable energy, and distributed generation. He was a recipient of several awards and honors, including the Service Merit Medal from Korean Government, the Young-Moon Park Best Scholar Award, and the Outstanding Scholar Award from the Korean Institute of Electrical Engineers.

YONG-TAE YOON (Member, IEEE) received the B.S., M. Eng., and Ph.D. degrees from the Massachusetts Institute of Technology (MIT), Cambridge, MA, USA, in 1995, 1997, and 2001, respectively. He is currently a Professor with the School of Electrical Engineering and Computer Science, Seoul National University, South Korea. His research interests include electric power network economics, power system reliability, and incentive regulation of independent transmission companies.